10

Acousto-Optic MultiBeam Axial Diffraction in Paratellurite

© S.N. Antonov[1], Yu.G. Rezvov[2¶], V.A. Podolsky[2], O.D. Sivkova[2]

[1] Kotelnikov Institute of Radio Engineering and Electronics, Russian Academy of Sciences, Fryazino Branch, Fryazino, Russia
[2] Mendeleev University of Chemical Technology of Russia, Novomoskovsk Institute (branch), Novomoskovsk, Tulskaya oblast, Russia
¶ E-mail: rezvovyug@mail.ru

Received May 6, 2021
Revised September 26, 2021
Accepted September 27, 2021

To form a multibeam radiation pattern, it is proposed to use the axial geometry of acousto-optic interaction in paratellurite. In the single frequency mode, the use of this geometry for angular scanning is characterized by a dip in the frequency response. Optimization of a multifrequency radio signal makes it possible to efficiently divide laser radiation into several beams with maintaining the fundamental advantages of axial geometry: minimum crystal size and power consumption.

Keywords: acousto-optic diffraction, acousto-optic deflector, axial geometry, multifrequency mode, paratellurite.

DOI: 10.21883/TPL.2022.01.52465.18860

The acousto-optics (AO) is based on the photoelastic effect occurring during the ultrasonic wave propagation in a transparent medium. The AO technologies are employed to control the optical radiation parameters in a wide wavelength range [1–6]. The fundamental advantages of AO devices are the possibility to control intense (up to hundreds of kW/cm^2) laser radiation, small induced light losses (of a few percent), high-speed response (tens of nanoseconds), absence of mechanically movable component parts, small dimensions and weight, low power consumption. The AO devices are used as modulators, angular scanners, light frequency shifters, multibeam field generators, etc.

Creation of high-power laser sources has set a task of dividing the laser beam into several independently controllable channels for the purpose of increasing the laser equipment efficiency, e. g., in the image displaying systems. The multibeam diffraction field may be generated by an AO device by feeding an optimized multifrequency radio signal [7–10].

The up-to-date applied AO is based mainly on a paratellurite crystal (TeO_2) possessing a phenomenally high AO efficiency. This enables creation of compact highly efficient devices with low energy consumption. This paper proposes to use in generating the multibeam field the known but rarely used variant of geometry of the AO interaction in paratellurite.

TeO_2 is the birefringent optically active and acoustically highly anisotropic crystal. The geometry (topology) of the AO interaction is commonly classified with respect to the sound direction relative to axis [110]. When the ultrasonic wave propagates with deflection from the axis, far-of-axis diffraction [11] takes place; if the sound propagates strictly along axis [110], and one of the interacting beams propagates along the optical axis, this is the case of axial diffraction (Fig. 1).

Here the sound (with wave vector $\mathbf{K}$) and incident light ($\mathbf{k}_{0e}$ means the extraordinary mode) are directed so that the diffracted light ($\mathbf{k}_{1o}$ means the ordinary mode) forms a right-angled triangle in the center of the range. The frequency

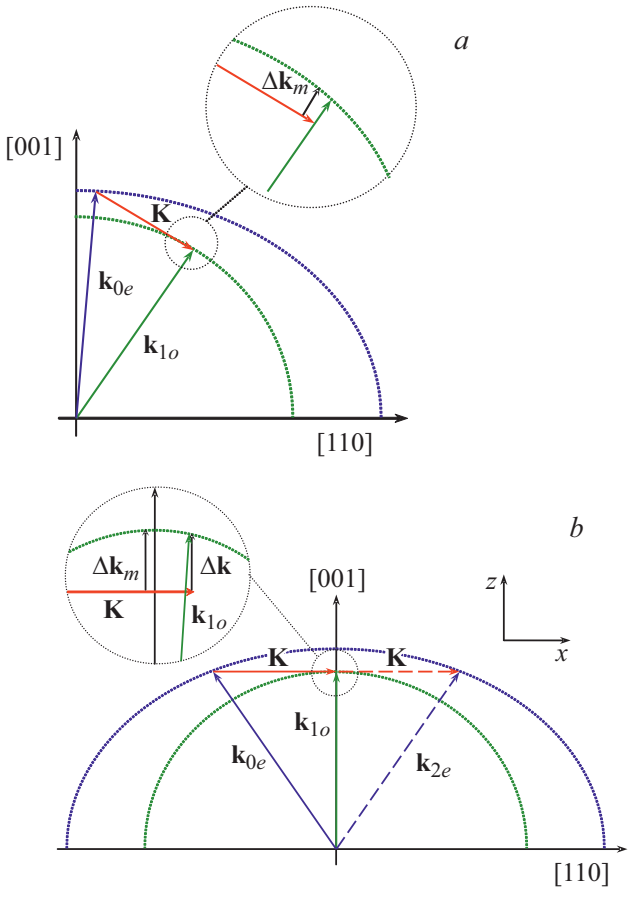

Figure 1. Vector diagram of the far-of-axis (*a*) and axial (*b*) diffraction types.

range may be extended by introducing misalignment $\Delta\mathbf{k}_m$ in the center of the transmission range.

The first-type diffraction is widely used in creating AO deflectors. However, the sound wave deflection from the [110] axis causes a decrease in the AO effective quality M_2 and makes it necessary to enlarge the crystal size along the [001] axis (because of the drift of acoustic energy). In the case of axial diffraction, the maximum value of M_2 is realized, while the crystal width depends only on the piezoelectric transducer size since ultrasound propagates without a drift. In this geometry, the diffraction without the polarization mode change is prohibited, therefore, the orders are formed according to the following scheme (digital symbols are the order numbers, alphabetic symbols characterize the polarization): $0e \to 1o \to 2e \to 3o \to 4e \ldots$.

In the plane-wave approximation, the set of equations describing the interaction of this type look as follows (axes x and z are shown in Fig. 1, *b*):

$$\frac{dC_0}{dZ} = -V^* C_1 \exp(-j\Delta_0 Z),$$

$$\frac{dC_1}{dZ} = VC_0 \exp(j\Delta_0 Z) - V^* C_2 \exp(-j\Delta_1 Z),$$

$$\frac{dC_2}{dZ} = VC_1 \exp(j\Delta_1 Z) - V^* C_3 \exp(-j\Delta_2 Z), \ldots.$$

Here C_0, C_1, C_2, C_3 are the relative amplitudes of orders $0e$, $1o$, $2e$, $3o$, etc. (the higher orders are usually truncated, the set being limited to the first three orders), $Z = z/L$ is the dimensionless interaction length. For the sake of compactness, designation $V = (\nu/2)\exp j\varphi$ is used, where ν is the Raman–Nath parameter, φ is the sound wave phase. Misalignments of orders are defined as $\Delta_0 = (k_{0z} - k_{1z})L$, $\Delta_1 = (k_{1z} - k_{2z})L, \ldots$ and are to be calculated taking into account conditions $k_{1x} = k_{0x} + K$, $k_{2x} = k_{1x} + K, \ldots$. The set of equations is to be solved with boundary conditions $C_0(0) = 1$, $C_1(0) = 0$, $C_2(0) = 0, \ldots$.

Hereinafter the calculations were performed at the light wavelength $\lambda = 0.63\,\mu$m, interaction length (the transducer width) $L = 5$ mm, and misalignment in the center $\Delta k_m L = 0.6$. Weak third and fourth orders were taken into account to estimate the energy loss.

The specific feature of this geometry is the presence of repeated diffraction (Fig. 1, *b*) giving rise to efficient energy transfer from the first diffraction order into the second one ($\mathbf{k}_{2e}$ means the extraordinary mode) [12,13]. Due to this, the first diffraction order efficiency drops in the center of the transmission band (Fig. 2, *a*). The diffraction efficiency increases with Raman–Nath parameter ν, being maximal in the transmission band center at $\nu_1 = \pi/\sqrt{2}$. In the case of accurate timing, this maximal value in the center of the range ($\Delta k_m L = 0$) is 50%, small misalignment $\Delta k_m L = 0.6$ reduces this value to 48%.

If the sound power continues increasing, the efficiency in the center decreases, efficiency beyond the dip increases and reaches its maximum at $\nu_2 = \pi$. The observed insignificant asymmetry is caused by deflection from the Bragg interaction mode and appearance of weak higher orders in the low-frequency part of the transmission band.

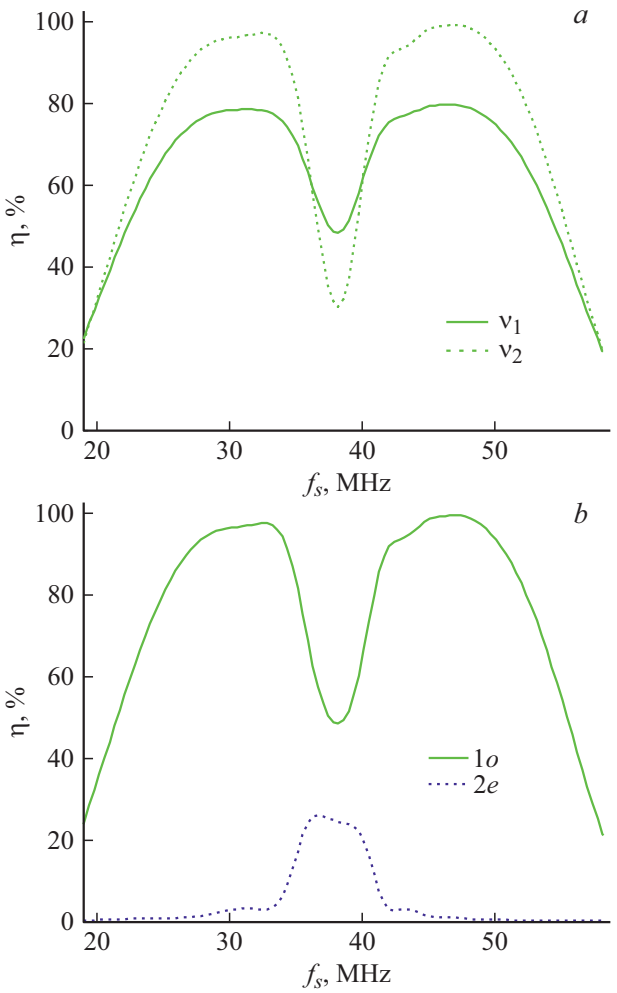

Figure 2. *a* efficiency of diffraction into the first (operating) diffraction order. The Raman–Nath parameter is $\nu_1 = \pi/\sqrt{2}$, $\nu_2 = \pi$. *b* intensities of the first ($1o$) and second ($2e$) order at the optimal acoustic power level.

As Fig. 2, *a* shows, the dip in the frequency response may be diminished by varying the sound power along with the frequency variation, i. e., by using such a mode when the Raman–Nath parameter is close to ν_1 in the center of the range and ν_2 far from the center. Relative efficiencies of the first and second orders obtained as a result of such optimization are presented in Fig. 2, *b*. The total efficiency of diffraction into higher orders does not exceed 1%.

The repeated diffraction restricts employment of the axial geometry for angular scanning (in the single-frequency mode). However, this type of diffraction is promising for laser systems exploiting the multibeam mode. According to the principles of the multibeam field formation, the diffraction efficiency at an individual frequency component separated out of the optimized radio signal is essentially lower than 100%. Hence, the effect of repeated diffraction may be considerably reduced, which will lead to an increase

in the total efficiency with retaining the advantages of this geometry.

Consider the diffraction on a radio signal consisting of a set of equidistant frequencies: f_0, $f_0 \pm \Delta f$, $f_0 \pm 2\Delta f, \ldots$. In this case, each order numbered m will be divided into a set of suborders with wave vectors $\mathbf{k}_{m,p}$ and relative amplitudes $C_{m,p}$ (p is the suborder number) at $k_{m,p+1,x} = k_{m,p,x} + 2\pi\Delta f/v_s$ (v_s is the sound speed).

The set of equations defining the evolution of suborders has the following form (with summation over the number of frequency components):

$$\frac{dC_{0,p}}{dZ} = -\sum_n V_n^* C_{1,p+n} \exp\left(-j\Delta_{0,p,p+n}Z\right),$$

$$\frac{dC_{1,p}}{dZ} = \sum_n V_n C_{0,p-n} \exp\left(j\Delta_{0,p-n,k}Z\right) - \sum_n V_n^* C_{2,p+n} \exp\left(-j\Delta_{1,p,p+n}Z\right),$$

$$\frac{dC_{2,p}}{dZ} = \sum_n V_n C_{1,p-n} \exp\left(j\Delta_{1,p-n,k}Z\right) - \sum_n V_n^* C_{3,p+n} \exp\left(-j\Delta_{2,p,p+n}Z\right), \ldots .$$

Here quantities $V_n = (v_n/2)\exp j\varphi_n$ are defined via the Raman–Nath parameter for the acoustic wave numbered n and phase φ_n. Misalignment between the suborder numbered p (in the order numbered m) and suborder numbered l (in the order numbered $m+1$) is defined as $\Delta_{m,p,l} = (k_{m,p,z} - k_{m+1,l,z})L$. At $Z = 0$, amplitudes of all the suborders are zero except for only one whose wave vector corresponds to the incident light (the corresponding amplitude is unity).

The calculation was performed for the radio signal consisting of five frequencies: f_0, $f_0 \pm \Delta f$, $f_0 \pm 2\Delta f$, where $f_0 = 38$ MHz is the range central part, $\Delta f = 6$ MHz is the frequency step. Behavior of nine suborders in each order was taken into account. The task was to maximally efficiently divide the incident light into five beams of equal intensities. It is known that realization of a specific multibeam pattern is possible at different phases of the radio signal components obeying several relations (the number of relations is less than the number of components), i. e., there is a great number of such realizations. Therefore, in the zero approximation there should be assigned Raman–Nath parameters v_n coarsely realizing the preset form and one set of phases φ_n minimizing intermodulation distortions. Later those parameters are being iteratively refined until the preset pattern is obtained.

This is the way in which one of the realizations was found. Fig. 3, *a* shows that the efficiency of diffraction into the first (operating) order on each individual component of a five-frequency optimized signal is 31–36%. For comparison, there is presented a frequency dependence of the efficiency of diffraction into the first order at $v = 1.3$ that is the value

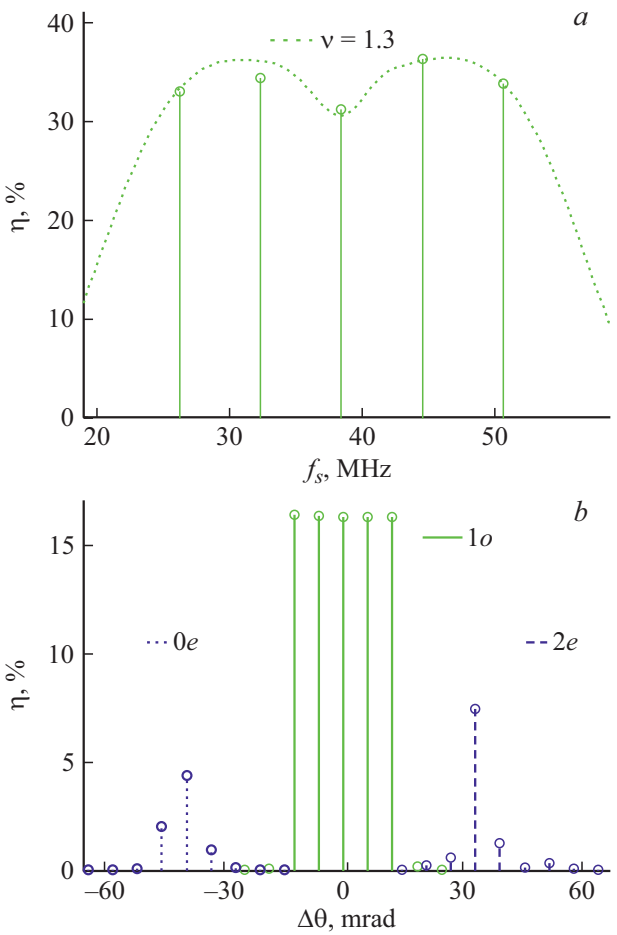

Figure 3. Diffraction efficiency at each individual component (*a*) and the multibeam pattern (with the angle counted from the pattern center in the first order) for the case of feeding a five-frequency optimized signal (*b*).

averaged over all the signal components. One can see that in this mode the dip in the center of the frequency response is slightly prominent.

The result of diffraction on the optimized signal is shown in Fig. 3, *b*. Complex intermodulation processes also divide the zero and second diffraction orders into suborders. In this case, in the transmitted light ($0e$) only about 8% of power persists, the most powerful suborder sustains less than 5%. The second order caused by the two-photon mechanism „takes off" 10% in total (less than 8% in the most remarkable suborder). In the first operating order, the equidistant and equally intense five-beam pattern is formed. Into each of five suborders, more than 16% of power of the incident radiation is deflected (more than 80% in total). Diffraction into higher diffraction orders is insignificant. Thus, in the first operating order a highly contrast five-beam field is formed with the total efficiency of above 80%.

Comparison of Figs. 3, *a* and *b* provides the illustration of the basic principle of the multibeam field formation with minimum losses. Usage of the optimized signal reduces

the efficiency of diffraction on each individual component (in our case, from 31–36% to 16%) with the increase in total efficiency into operating suborders and simultaneous suppression of intermodulation suborders. In [9], such calculations were performed in the far-of-axis geometry and predicted the total five-beam field efficiency of almost 100% in a wide range of the frequency step Δf. In the same study, formation of such a field with the efficiency of 95% was shown experimentally. Thus, the use of the axial geometry instead of far-of-axis one results in reducing the maximum efficiency of the multibeam field (in our case, to 80%). The effect of the efficiency reduction has to depend on the frequency component positions in the transmission band.

What is important is the extent of reasonability of using the plane-wave approximation. The slow transverse mode excited in paratellurite at a small angle to axis [110] possesses high diffraction divergence coefficients. This „approximates" the typical diffraction structure of the ultrasonic beam tens of times closer (as compared with the isotropic medium) at the same lateral dimensions. However, the results of [9] show that when the laser beam propagates with the aperture less than 1 mm (the sound being directed at the angle of 6° to axis [110], the frequency range being 20–50 MHz) in the sound field region adjoining the transducer, the plane-wave approximation is quite adequate. The same accuracy of this approximation may be expected also in the axial geometry at the comparable ultrasonic beam lateral dimensions, sound frequency and light aperture.

The obtained results show that the axial geometry in paratellurite, which is actually not used to deflect the incident radiation into one operating order, is quite promising for forming a multibeam radiation pattern. In this case, the total useful efficiency of diffraction exceeds the 50% level that is maximal in the single-beam mode. Hence, the axial geometry can find application in systems of laser processing of materials due to its fundamental advantages: minimum crystal size and power consumption.

Acknowledgements

The authors are grateful to the Andrey Melnichenko Foundation for the help in accomplishing this study.

Financial support

The study was supported by the State Budget according to State Assignment 0030-2019-0014.

Conflict of interests

The authors declare that they have no conflict of interests.

References

[1] L.N. Magdich, V.Ya. Molchanov, *Acoustooptic devices and their applications* (Gordon and Breach, N.Y., 1989).
[2] V.I. Balakshy, V.N. Parygin, L.E. Chirkov, *Fizicheskie osnovy akustooptiki* (Radio i svyaz', M., 1985) (in Russian).
[3] A. Korpel, *Acousto-optics* (Marcel Dekker, N.Y., 1988).
[4] J. Xu, R. Stroud, *Acousto-optic devices* (Wiley, N.Y., 1992).
[5] *Design and fabrication of acousto-optic devices*, ed. by A.P. Goutzoulis, D.R. Pape (Marcel Dekker, N.Y., 1988).
[6] V.Ya. Molchanov, Yu.I. Kitaev, A.I. Kolesnikov, V.N. Narver, A.Z. Rozenshtein, N.P. Solodovnikov, K.G. Shapovalenko, *Teoriya i praktika sovremennoy akustiki* (MISiS, M., 2015) (in Russian).
[7] S.N. Antonov, Y.G. Rezvov, Instrum. Exp. Tech., **63** (6), 835 (2020). DOI: 10.1134/S0020441220050267.
[8] S.N. Antonov, Yu.G. Rezvov, Tech. Phys., **52** (8), 1053 (2007). DOI: 10.1134/S1063784207080154.
[9] S.N. Antonov, A.V. Vainer, V.V. Proklov, Yu.G. Rezvov, Tech. Phys., **53** (6), 752 (2008). http://journals.ioffe.ru/articles/9437 DOI: 10.1134/S1063784208060145.
[10] S.N. Antonov, A.V. Vainer, Y.Y. Gubareva, L.F. Kupchenko, V.V. Proklov, Yu.G. Rezvov, Tech. Phys. Lett., **37** (6), 530 (2011). journals.ioffe.ru/articles/12582 DOI: 10.1134/S1063785011060022.
[11] T. Yano, M. Kawabuchi, A. Fukumoto, A. Watanabe, Appl. Phys. Lett., **26** (12), 689 (1975). DOI: 10.1063/1.88037
[12] A.W. Warner, D.L. White, W.A. Bonner, J. Appl. Phys., **43** (11), 4489 (1972). DOI: 10.1063/1.1660950
[13] A.V. Zakharov, V.B. Voloshinov, Tech. Phys., **61** (9), 1377 (2016). http://journals.ioffe.ru/articles/43561 DOI: 10.1134/S1063784216090292.